INSTITUTE OF PHYSICS PUBLISHING MEASUREMENT SCIENCE AND TECHNOLOGY
Meas. Sci. Technol. **12** (2001) 1365–1370 www.iop.org/Journals/mt PII: S0957-0233(01)20787-5

A plasma cloud charge sensor for pulse keyhole process control

Y M Zhang, S B Zhang and Y C Liu

Department of Electrical and Computer Engineering and Center for Robotics and Manufacturing Systems, College of Engineering, University of Kentucky, Lexington, KY 40506, USA

Received 11 January 2001, accepted for publication 30 April 2001

Abstract
Keyhole plasma arc welding achieves much deeper penetration than do all other existing arc welding processes. Because of its ability to penetrate thicker material, the control of the keyhole in plasma arc welding becomes critical. From an analysis of the physical process, a sensor to detect the state of the keyhole for keyhole process control has been proposed and developed. This sensor measures the electrical effect of the plasma cloud generated during keyhole plasma arc welding. It is found that the plasma cloud, which rapidly decreases to zero upon establishment of the fully penetrated keyhole, can be used to detect the state of the keyhole reliably. The effectiveness of the proposed sensor for detecting the keyhole state has been verified during pulse keyhole plasma arc welding.

Keywords: arc, plasma, welding

1. Introduction

Keyhole plasma arc welding (PAW) achieves much deeper penetration than do all other existing arc welding processes [1]. However, to maintain a fully penetrated keyhole continuously, a large current has to be applied in order to provide a sufficient plasma pressure against the surface tension and the hydrostatic head [2, 3]. Since too large a pressure also blows the liquid metal away from the weld pool, it may be preferable that the welding current be decreased in order to reduce the blowing force after the establishment of the keyhole has been detected. Such a decrease in the welding current can also help to reduce the heat input. Of course, the decrease in the welding current will cause the keyhole to close. To achieve full penetration, the fully penetrated keyhole has to be re-established. As a result, a pulse keyhole process can be used to decrease the blowing force and the heat input, while the desired full penetration is also ensured by the periodic establishment of the fully penetrated keyhole. It was also found that such a pulse keyhole is critical in controlling the melt metal during double-sided arc welding, which can penetrate a 12.7 mm thick square butt joint in a single pass [4]. Of course, to implement this pulse keyhole process, detection of the keyhole is fundamental.

Detection of the fully penetrated keyhole has attracted the interest of researchers. An early study monitored the light of the plasma efflux from the keyhole [2]. Of course, this method required access to the back side of the workpiece, which is not always available. In another study, spectral lines of hydrogen and argon were monitored from the front side to determine the establishment of the fully penetrated keyhole [5]. Although it required no access to the back side of the workpiece, its implementation was complicated by the need for a photosensor to monitor spectral lines. It is evident that the welding industry prefers simpler and more reliable sensors.

The fundamental physical characteristics of welding arcs may offer mechanisms on the basis of which one can develop simple, robust and reliable solutions, as can be seen in penetration sensing [6, 7]. During keyhole PAW, the weld pool is subject to the impact of the high-speed, high-density plasma jet which forms a funnel-shaped cavity referred to as the keyhole [8–10]. The flow of the plasma jet within the keyhole, be it unpenetrated or fully penetrated, is governed by mass, momentum and energy conservation laws with the geometry of the keyhole providing the boundary conditions [11–13]. The development of the keyhole determines the dynamic behaviour of the plasma jet. Hence, monitoring the behaviour of the plasma jet may provide an effective method for detecting the development or the state of the keyhole. As a result, in this study we intend to develop a keyhole sensor, referred to as the plasma cloud charge sensor, which monitors the charge effect of the dynamic change of the plasma cloud above the surface of the workpiece.

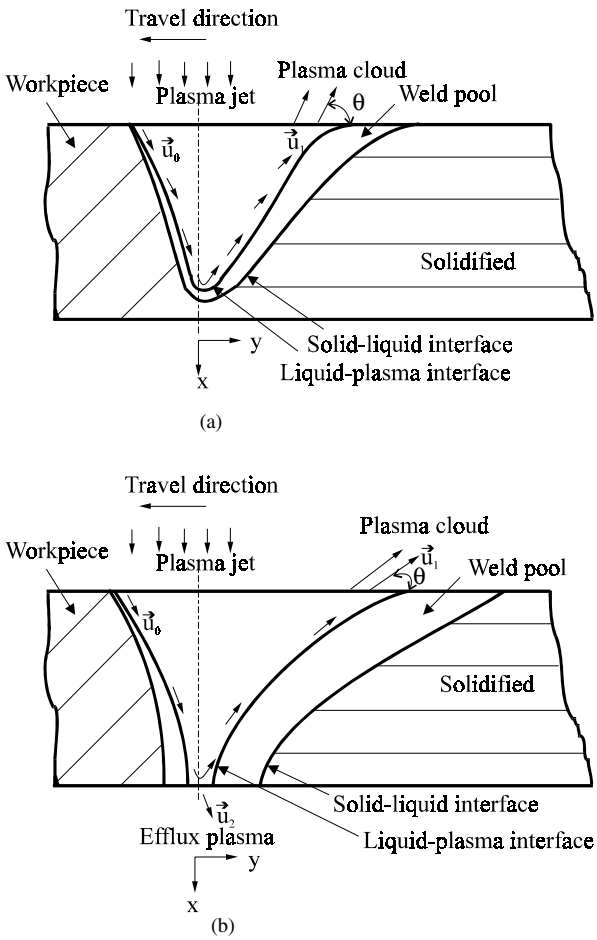

Figure 1. The plasma-jet flow model within a moving keyhole: (*a*) an unpenetrated keyhole and (*b*) a fully penetrated keyhole.

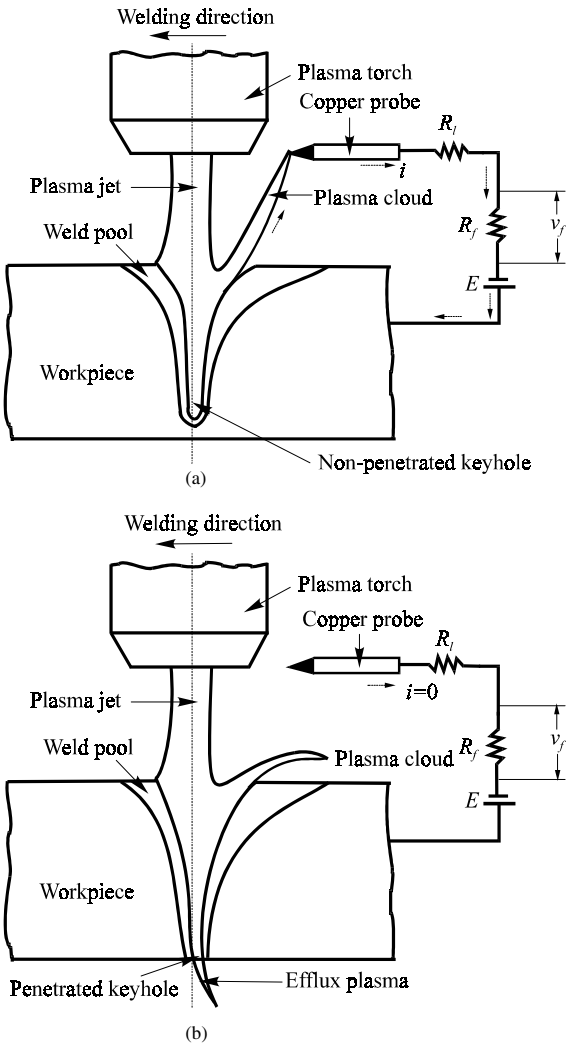

Figure 2. A schematic view of measurement using the PCCS: (*a*) an unpenetrated keyhole and (*b*) a fully penetrated keyhole.

2. The principle

The mass continuity [11, 14] suggests that, before the fully penetrated keyhole is established, the flux of plasma flowing into the cavity must equal the flow out of the cavity. For a moving keyhole, because the high-velocity plasma jet hits the front wall of the keyhole, the rear portion of the keyhole is not subject to effects of the plasma jet. The flow of a plasma jet within the keyhole is shown in figure 1(*a*). Neglecting the metal vapour, the mass continuity equation becomes

$$\rho_0 u_0 = \rho_1 u_1 \tag{1}$$

where ρ_0 and u_0 are the density of the plasma and the velocity of the flow going into the keyhole, whereas ρ_1 and u_1 are the density of plasma and the velocity of the flow coming out of the keyhole. Hence, from the law of conservation of mass, it must occur that the plasma jet flows out of the cavity from the top side of the unpenetrated keyhole to form a plasma cloud. On the other hand, when a fully penetrated keyhole is established, the state variables of the system, such as the temperature, pressure, velocity and density of plasma, change significantly (figure 1(*b*)). The mass continuity equation for a fully penetrated keyhole can be expressed as

$$\rho_0 u_0 = \rho_1' u_1' + \rho_2' u_2' \tag{2}$$

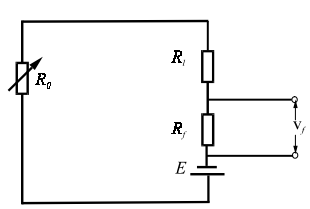

Figure 3. The equivalent circuit of the PCCS.

where ρ_1' and u_1' are the density of plasma and velocity of the flow coming out of the keyhole from the top side, whereas ρ_2' and u_2' are the density of plasma and velocity of the flow coming out of the keyhole from the back side. Hence, due to the establishment of the fully penetrated keyhole, part of the plasma flows out of the keyhole from the back side. That is, $\rho_1' u_1' < \rho_1 u_1$. Monitoring the plasma cloud from the top side during plasma arc welding can thus detect the existence and the establishment of the fully penetrated keyhole. Hence, a plasma cloud charge sensor (PCCS) to monitor the variation in the plasma cloud can be proposed. For simplicity and robustness, the PCCS will be designed on the basis of an electronic probe technique [15].

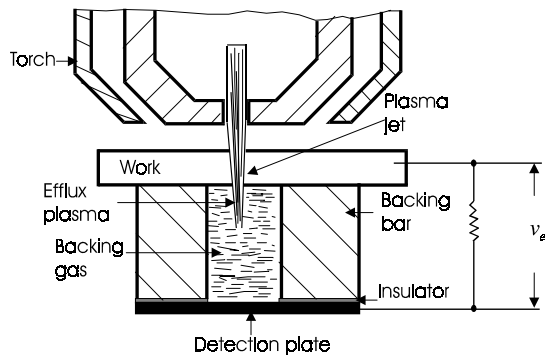

Figure 4. A schematic view of measurement using the EPCS.

3. The sensor

The proposed PCCS consists of a copper probe, a shielding cup and a measurement circuit (figure 2). The copper probe is mounted inside the shielding cup and placed behind the plasma torch and above the workpiece (figure 2). It is electrically isolated from the plasma electrode and is connected to the measurement circuit. The measurement circuit consists of a resistance R_f (5 Ω), a voltage ($V_0 = 15$ V) source and a resistance R_l (5 Ω) which restricts the current. The output signal of the sensor, v_f measured across R_f, is recorded by a data acquisition system.

The ionized plasma cloud functions as an electrical passage to close the measurement circuit. Its conductivity is determined by the temperature of the plasma cloud and the density of the electrons in the plasma cloud [16]. Hence, R_0, the equivalent resistance of the electrical passage established by the plasma cloud, is mainly controlled by the density of the electrons when the temperature is given. That is, R_0 is dependent on the degree of ionization and the density of the electrons. When the degree of ionization of the plasma cloud is approximately fixed, measuring R_0 could be an effective way of estimating the density of the plasma cloud and thus the state of penetration of the keyhole.

The equivalent measurement circuit is shown in figure 3. The voltage v_f across R_f is

$$v_f = \frac{V_0 R_e}{R_0 + R_e + R_l}. \tag{3}$$

Hence, when the plasma cloud is strong, such as during periods with an unpenetrated keyhole, v_f is strong because of the small R_0. After the fully penetrated keyhole has been established, the plasma cloud becomes very weak. The resultant R_0 will be very large, such that the output signal v_f of the sensor decreases nearly to zero. Hence, v_f may be used to detect the state of the keyhole, i.e. unpenetrated or fully penetrated, reliably.

To verify the effectiveness of the PCCS for detecting the state of the keyhole, another sensor which measures the efflux

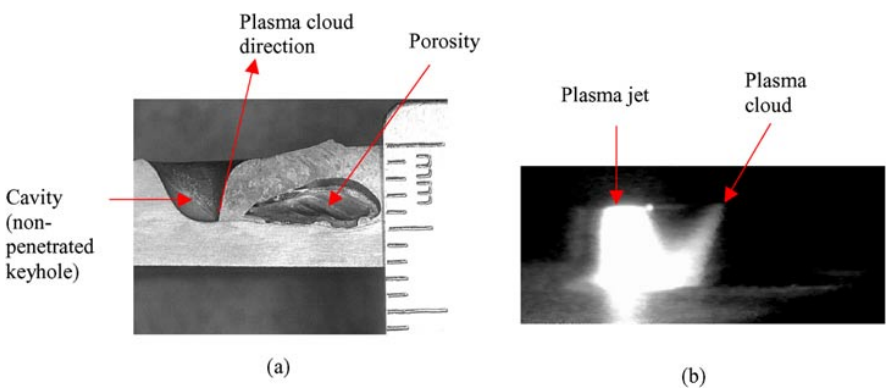

Figure 5. The keyhole and plasma cloud at high travelling speed: (*a*) an unpenetrated keyhole and (*b*) a plasma jet and a strong plasma cloud.

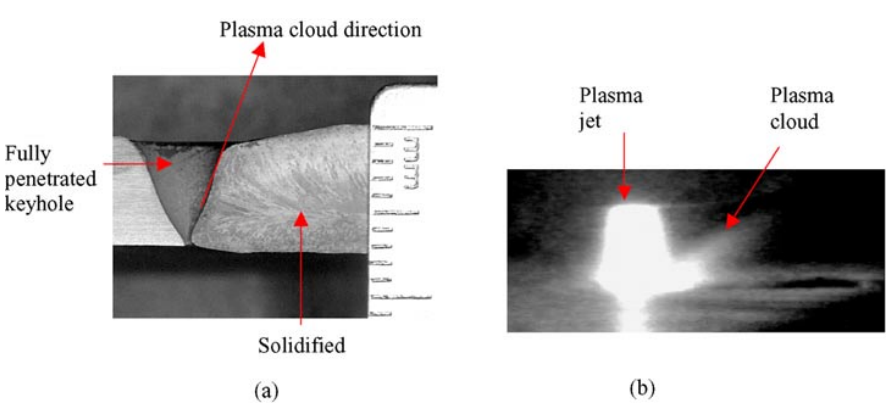

Figure 6. The keyhole and plasma cloud at medium travelling speed: (*a*) a fully penetrated keyhole and (*b*) a plasma jet and a plasma cloud.

plasma from the back side of the workpiece as shown in figure 4 and introduced in [17] has been employed. This verification sensor, referred to as an efflux plasma charge sensor (EPCS) [17], gives a non-zero output when and only when the keyhole is penetrated such that the efflux plasma charges a voltage v_e between the electrically isolated workpiece and the detection plate. When the keyhole is not fully penetrated, there is no efflux plasma between the workpiece and the detection plate. The output signal v_e thus must be zero.

4. The keyhole mode and the plasma cloud

To investigate the relationship between the plasma cloud and the shape of the keyhole, the welding current has suddenly been switched to zero to freeze the keyhole, as had been done previously [18]. Because of the pressure and the fast cooling of the plasma gas, this method can firmly maintain the shape of the keyhole after the current has been switched to zero if the weld pool is not very large. Hence, the shape of the keyhole prior to the switching may then be measured off-line. Also, the dynamics of the plasma cloud can be monitored by a CCD camera assisted by a laser beam as background light. As a result, data can be obtained in order to study the behaviour of the plasma cloud with variations in shape of the keyhole.

We performed a series of tests. In these tests, the plasma current was 100 A. Three levels of travelling speed, high (3 mm s^{-1}), medium (2.3 mm s^{-1}) and low (1.5 mm s^{-1}), were used to establish different steady-state keyholes. At high speed, the keyhole was not penetrated (figure 5(*a*)). In this case, the plasma cloud was very strong (figure 5(*b*)) and the deflection angle θ was large (figure 5(*a*)). As shown in figure 5(*b*), the rear edge of the longitudinal section of the cavity (unpenetrated keyhole) was very steep. This matches the large deflection angle of the plasma cloud. When the travelling speed was reduced to 2.3 mm s^{-1}, a fully penetrated keyhole was established (figure 6(*a*)). The intensity and the deflection angle of the plasma cloud both decreased significantly, as can be seen in figure 6(*a*) and (*b*). Also, the slope of the rear edge of the fully penetrated keyhole decreased significantly (figure 6(*a*)). With a further reduction of the travelling speed to 1.5 mm s^{-1}, the state of penetration of the keyhole was further improved. In this case, there was sagging of the back side of the weld (figure 7(*a*)) due to the larger exit opening of the fully penetrated keyhole. However, in this case, the keyhole was not successfully frozen. (This lack of success in freezing the keyhole may have been caused by the large weld pool which cools and freezes slowly.) Hence, as shown in the estimated keyhole given in figure 7(*b*), the improvement of the state of penetration of the keyhole further reduced the slope of the rear edge (figure 7(*a*)). The plasma cloud became too small and too low to be observed (figure 7(*c*)).

5. Monitoring and verification

It is evident that the intensity and deflection angle of the plasma cloud are dependent on the state (shape) of the keyhole. It is possible to monitor the state of the keyhole by monitoring the plasma cloud for real-time control of pulse keyhole PAW.

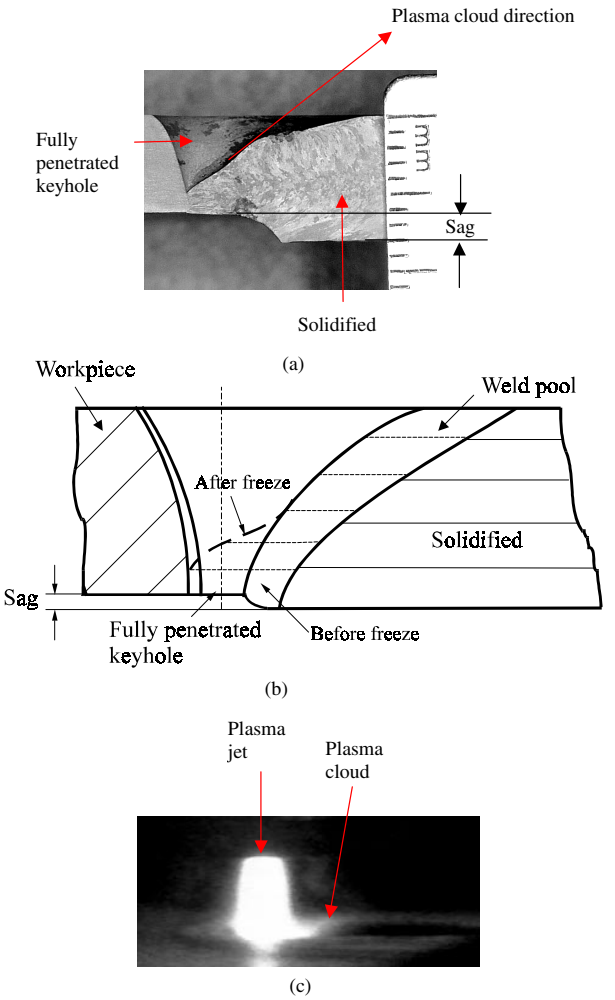

Figure 7. The keyhole and plasma cloud at low travelling speed: (*a*) a frozen section, (*b*) an estimated longitude section and (*c*) a plasma jet and a plasma cloud.

To verify this feasibility, experiments have been done. Both 6.4 and 9.5 mm thick stainless steel plates were pulse keyhole plasma arc welded using the welding parameters listed in table 1. As can be seen in figure 8, the PCCS signal v_f becomes strong after the current is switched from the base level (50 A) to the peak level (140 A). However, despite the peak current, the EPCS signal v_e is zero when v_f is strong. It is known that a large v_f indicates that there is a strong plasma cloud and that zero v_e implies that no fully penetrated keyhole has been established. That is, the plasma cloud signal v_f successfully detects the state of the keyhole before the fully penetrated keyhole is established. Furthermore, figure 8 shows that v_f decreases nearly to zero and v_e becomes non-zero at approximately the same time. Hence, the EPCS signal also verified that the plasma cloud signal is capable of detecting the establishment of the fully penetrated keyhole.

6. Sensitivity and accuracy

The above experiments verified the effectiveness of the proposed PCCS. However, the sensitivity and accuracy of the

Table 1. Welding parameters.

Thickness	6.4 mm (1/4 inch)	9.5 mm (3/8 inch)
Peak current	140 A	200 A
Peak period	60 ms	30 ms
Base current	50 A	85 A
Base period	80 ms	80 ms
Travel speed	2.2 mm s^{-1}	2.0 mm s^{-1}
Orifice diameter	2 mm (0.78 inch)	2.8 mm (0.11 inch)
Plasma gas	4 scfh	4.8 scfh
Shielding gas	30 scfh	30 scfh
Backing gas	30 scfh	30 cfh
Stand-off	6 mm (0.24 inch)	6 mm (0.24 inch)

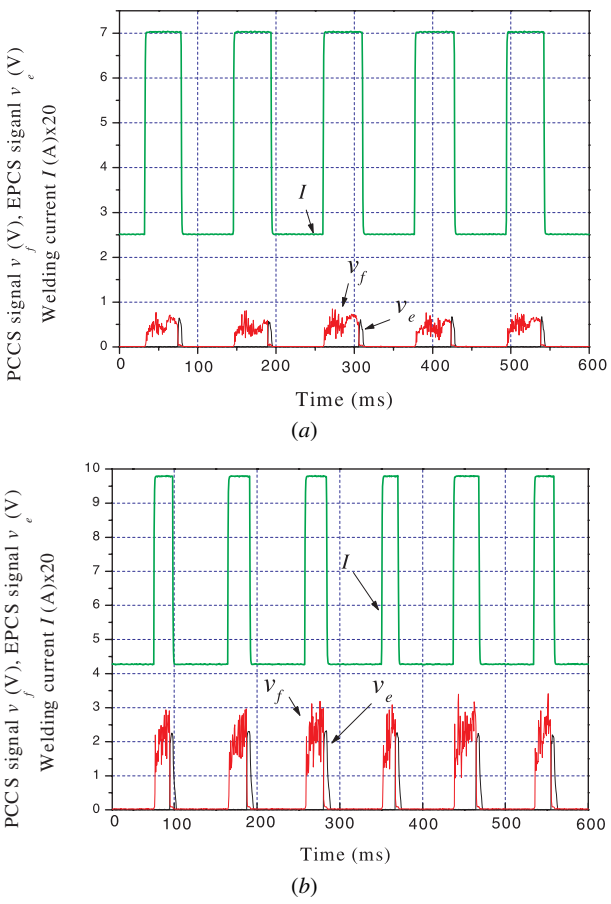

Figure 8. Measurements during pulse keyhole plasma arc welding: (*a*) 6.4 mm thick butt joint and (*b*) 9.5 mm thick butt joint.

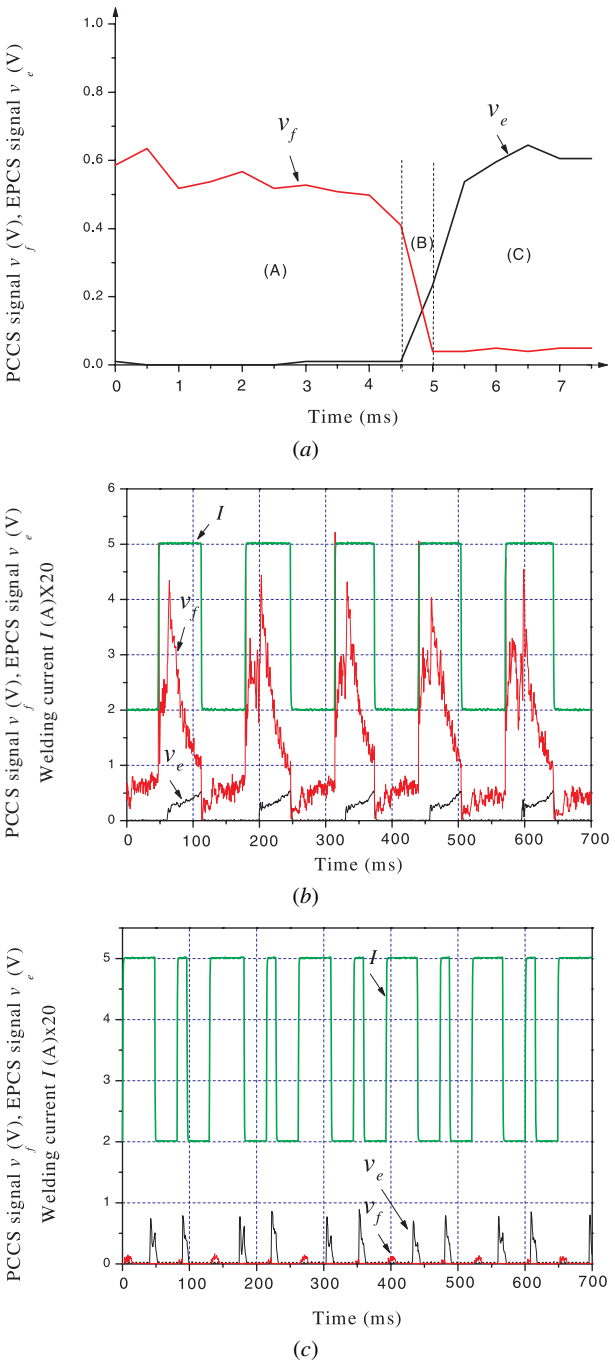

Figure 9. Monitoring keyhole formation from various probe locations: (*a*) $d = 10$ mm, $h = 5$ mm, (*b*) $d = 5$ mm, $h = 2$ mm and (*c*) $d = 15$ mm, $h = 8$ mm.

PCCS for sensing the plasma cloud for the detection of the fully penetrated keyhole depend on the location of the probe which is specified by its distance from the axis of the electrode (d) and its distance from the surface of the workpiece (h). To study the influence of the location, 6.4 mm thick stainless steel plates were butt welded. The EPCS signal v_e was measured simultaneously with the PCCS signal v_f.

Figure 9(*a*) shows the signals measured when $d = 10$ mm and $h = 5$ mm. As can be seen in figure 9(*a*), in region (A), v_e is zero and v_f is strong. They both suggest that the keyhole has not been penetrated. In region (B), v_f quickly drops nearly to zero and v_e rapidly increases from zero. The establishment of the fully penetrated keyhole was detected by both signals. In region (C), v_f becomes very weak due to the establishment of the fully penetrated keyhole, which is verified by the strong efflux plasma charge signal v_e. It can be seen that the PCCS has not only detected the keyhole state accurately but also predicted the establishment of the penetrated keyhole approximately 0.5 ms in advance of the EPCS. Of course, this advance is quite understandable because the EPCS does not respond until the fully penetrated state of the keyhole has completely been established.

It can be seen that the location ($d = 10$ mm, $h = 5$ mm) gives an accurate detection of the state of the keyhole. If the

distance between the electrode and the probe is decreased to 5 mm such that $d = 5$ mm and $h = 2$ mm, v_f does not drop to zero after the EPCS signal v_e has indicated the establishment of the fully penetrated keyhole (figure 9(*b*)). In this case, in addition to the plasma cloud deflected from the keyhole, the plasma jet also contributes to v_f because of the small distance between the probe and the plasma jet. Hence, to make analysis of the signal easier, the probe should be at a sufficient distance from the plasma jet that v_f drops nearly to zero when the fully penetrated keyhole is established.

Of course, if the probe is too high above the surface or too far from the axis of the electrode for the plasma cloud to reach, the signal v_f will be too weak to be utilized to detect the state of the keyhole. As can be seen in figure 9(*c*), when $d = 15$ mm and $h = 8$ mm, v_f becomes very weak. The sensitivity of the sensor is not sufficient.

Experiments showed that 8–12 mm and 3–6 mm are the appropriate ranges from the distance between the probe and the axis of the electrode and the distance between the probe and the surface of the workpiece, respectively. Within these ranges, the sensitivity and accuracy of the sensor are sufficient to detect the state of the keyhole. In addition, the probe is at a sufficient distance from the plasma jet and the workpiece to avoid the possibility of overheating and collision.

7. Conclusions

(i) The proposed PCCS is based on the mass continuity and the conductivity of the ionized plasma cloud. The mechanism involved in the sensing principle ensures the reliability of the sensor.

(ii) The proposed probe and measurement circuit make it possible to attach the sensor to the welding torch to form a desired compact sensor which requires no access to the back side of the workpiece. It is evident that such a sensor is insensitive to the arc radiation and the variable surface conditions and is much more robust than other sensors such as CCD cameras.

(iii) Experiments have verified the effectiveness of the proposed sensor for detecting the state of the keyhole and its capability in pulse keyhole process control. However, to maximize the robustness and accuracy of the sensor, the probe must be placed appropriately. Under the welding conditions in this study, it is recommended that the probe be 3–6 mm above the workpiece and 8–12 mm behind the axis of the electrode.

Acknowledgment

This work is funded by the National Science Foundation of the USA under grant DMI-9812981 and the Center for Robotics and Manufacturing Systems.

References

[1] 1990 *Welding Handbook* vol 2, 8th edn (Miami: American Welding Society)

[2] Metcalfe J C and Quigley M B C 1975 Keyhole stability in plasma arc welding *Welding J.* **54** 401–4

[3] Keanini R G and Rubinsky B 1990 Plasma arc welding under normal and zero gravity *Welding J.* **69** 41–50

[4] Zhang Y M, Zhang S B, Jiang M and Losch B 2001 Sensing and control of double-sided arc welding process *Proc. 2001 National Science Foundation Design, Service and Manufacturing Grantees and Research Conf. (Tampa, FL, 7–10 January 2001)*

[5] Martinez L F, Marques R E, Mcclure J C and Nunes J R 1993 Front side keyhole detection in aluminum alloys *Welding J.* **72** 49–51

[6] Bicknell A, Smith J S and Lucas J 1994 Arc voltage sensor for monitoring of penetration in TIG welds *Proc. IEE* **141** 513–20

[7] Aendenroomer A J R and den Ouden G 1998 Welding pool oscillation as a tool for penetration sensing during pulsed GTA welding *Welding J.* **77** 181–7

[8] Keanini G R and Rubinsky B 1993 Three-dimensional simulation of the plasma arc welding process *Int. J. Heat Mass Transfer* **36** 3283–98

[9] Lancaster J F 1986 *The Physics of Welding* (Oxford: Pergamon) 307–18

[10] Steffens H D and Kayser H 1972 Automatic control for plasma arc welding *Welding J.* **51** 408–17

[11] Imrie B W 1973 *Compressible Fluid Flow* (London: Butterworth) pp 1–19

[12] Aris R 1962 *Vectors, Tensors and the Basic Equations of Fluid Mechanics* (New York: Dover)

[13] Boulos M, Fauchais P and Pfender E 1994 *Thermal Plasma: Fundamentals and Application* vol 1 (New York: Plenum)

[14] Lowke J J, Morrow R and Haidar J 1997 A simplified unified theory of arcs and their electrodes *J. Phys. D: Appl. Phys.* **30** 2033–42

[15] Swift J D and Schwar M J R 1970 *Electrical Probes for Plasma Diagnostics* (London: Iliffe)

[16] Cambel A B 1963 *Plasma Physics and Magnetofluid-mechanism* (New York: McGraw-Hill) pp 152–91

[17] Zhang S B and Zhang Y M 2001 Efflux plasma charge based sensing and control of joint penetration during keyhole plasma arc welding *Welding J. Res. Suppl.* **80** (7) at press

[18] Tomsic M J and Jackson C E 1974 Energy distribution in keyhole mode plasma arc welds *Welding J.* **53** 109–15